High resolution NMR study of T1 magnetic relaxation dispersion. III. Influence of spin 1/2 hetero-nuclei on spin relaxation and polarization transfer among strongly coupled protons

Sergey E. Korchak, Konstantin L. Ivanov, Andrey N. Pravdivtsev, Alexandra V. Yurkovskaya, Robert Kaptein, and Hans-Martin Vieth

High resolution NMR study of T_1 magnetic relaxation dispersion. III. Influence of spin 1/2 hetero-nuclei on spin relaxation and polarization transfer among strongly coupled protons

Sergey E. Korchak,[1,2] Konstantin L. Ivanov,[3,4] Andrey N. Pravdivtsev,[3,4] Alexandra V. Yurkovskaya,[3,4] Robert Kaptein,[4,5] and Hans-Martin Vieth[1,a)]

[1]*Institut für Experimentalphysik, Freie Universität Berlin Arnimallee 14, 14195 Berlin, Germany*
[2]*Physikalisch-Technische Bundesanstalt, Abbestr. 2-12, 10587 Berlin, Germany*
[3]*International Tomography Center, Institutskaya 3a, Novosibirsk 630090, Russia*
[4]*Novosibirsk State University, Pirogova 2, Novosibirsk 630090, Russia*
[5]*Bijvoet Center, Utrecht University, Padualaan 8, 3584 CH Utrecht, The Netherlands*

Effects of spin-spin interactions on the nuclear magnetic relaxation dispersion (NMRD) of protons were studied in a situation where spin $\frac{1}{2}$ hetero-nuclei are present in the molecule. As in earlier works [K. L. Ivanov, A. V. Yurkovskaya, and H.-M. Vieth, J. Chem. Phys. **129**, 234513 (2008); S. E. Korchak, K. L. Ivanov, A. V. Yurkovskaya, and H.-M. Vieth, *ibid.* **133**, 194502 (2010)], spin-spin interactions have a pronounced effect on the relaxivity tending to equalize the longitudinal relaxation times once the spins become strongly coupled at a sufficiently low magnetic field. In addition, we have found influence of ^{19}F nuclei on the proton NMRD, although in the whole field range, studied protons and fluorine spins were only weakly coupled. In particular, pronounced features in the proton NMRD were found; but each feature was predominantly observed only for particular spin states of the hetero-nuclei. The features are explained theoretically; it is shown that hetero-nuclei can affect the proton NMRD even in the limit of weak coupling when (i) protons are coupled strongly and (ii) have spin-spin interactions of different strengths with the hetero-nuclei. We also show that by choosing the proper magnetic field strength, one can selectively transfer proton spin magnetization between spectral components of choice. © *2012 American Institute of Physics.* [http://dx.doi.org/10.1063/1.4746780]

I. INTRODUCTION

Field-cycling NMR relaxometry is a well-established method for probing molecular mobility in a wide range of systems, most notably, in liquid solutions, polymers, molecular crystals, proteins, and other biomolecules.[1–11] In field-cycling NMR experiments, the nuclear magnetic relaxation dispersion (NMRD) curve is measured, which is the magnetic field dependence of the longitudinal relaxation rate, R_1, i.e., the inverse of the longitudinal relaxation time, T_1: $R_1 = 1/T_1$. In general, the rate of the relaxation transition between the μ-th and ν-th levels, $R_{\mu\nu}$ is given in second-order perturbation theory by[12]

$$R_{\mu\nu} = \int_0^\infty \overline{V_{\mu\nu}(t)V_{\nu\mu}(t+\tau)}e^{i\omega_{\nu\mu}\tau}d\tau$$
$$+ \int_0^\infty \overline{V_{\nu\mu}(t)V_{\mu\nu}(t+\tau)}e^{-i\omega_{\nu\mu}\tau}d\tau. \tag{1}$$

Here, $\omega_{\mu\nu}$ stands for the transition frequency (energy difference between states $|\mu\rangle$ and $|\nu\rangle$), $V_{\mu\nu}$ and $V_{\nu\mu}$ denote the matrix elements of the fluctuating Hamiltonian responsible for the relaxation; averaging is performed over the spin ensemble (i.e., different fluctuations). The expression for $R_{\mu\nu}$ becomes simpler when the fluctuations can be written as the product

of time-dependent functions, f_n, with auto-correlation functions, $G_n(\tau) = \overline{f_n(t)f_n(t+\tau)}$, and time-independent spin operators, $\hat{A}^{(n)}$. Then the relaxation rate is as follows:

$$R_{\mu\nu} = 2\sum_n \left|A_{\mu\nu}^{(n)}\right|^2 J_n(\omega_{\mu\nu}),$$

$$\text{where} \quad J_n(\omega) = \int_0^\infty G_n(t)e^{-i\omega t}dt. \tag{2}$$

Thus, any relaxation rate (including R_1) can be magnetic field dependent for three reasons. First, $J(\omega)$ changes with the external magnetic field strength since ω usually is field dependent. In the case of longitudinal relaxation of a single spin species, ω is directly proportional to the field: $\omega = \gamma B$. Hence, measurement of the magnetic field dependence of R_1 allows one to determine $J(\omega)$ and from that the correlation times, τ_c, of molecular motion. This procedure is complicated when not only $J(\omega)$ is field-dependent but also the spin operators $\hat{A}^{(n)}$ (e.g., for relaxation caused by chemical shift anisotropy), which is a second factor for the field-dependence of R_1 rates. The relaxation dispersion may be affected by an additional third factor when the eigen-functions, $|\mu\rangle$ and $|\nu\rangle$, of the Hamiltonian show a field dependence. Because of this the matrix elements $|A_{\mu\nu}^{(n)}|^2$ change with the field even when the operators $\hat{A}^{(n)}$ are field-independent. Usually, only the first two factors are taken into consideration for the field dependence of the relaxation rates. However, the third factor may become

a)Author to whom correspondence should be addressed. Electronic mail: hans-martin.vieth@physik.fu-berlin.de. FAX: +49-30-83856081.

important in the presence of spin-spin couplings among the relaxing spins. They may vary the spin eigen-states with the field and cause pronounced changes in the relaxation behavior. Experimental studies of the third factor are limited by the fact that (with very few exceptions[13–18]) the experimental methods are lacking NMR spectral resolution and therefore allow one to investigate only the relaxation of the total magnetization of solvent or solute molecules. Such studies are unable to directly identify the consequence of spin-spin interactions.

In recent works, we have demonstrated theoretically and experimentally that in scalar coupled spin systems there are pronounced features in NMRD related to field dependent eigen-functions of the spin system.[13, 14, 19] Although the strength of spin-spin interactions is quite small (not larger than 30 Hz for protons) as compared to the large Zeeman interactions with the magnetic field (often reaching hundreds of MHz), these couplings can strongly affect the eigen-states of the spin system and thus cause a field dependence of the R_1 rates. The features observed are caused by the fact that at low magnetic fields the spins reach the regime of strong coupling. This is the case when the difference of the Zeeman interactions of spins, ν_i and ν_j, becomes smaller than their spin-spin interaction, J_{ij}:

$$|\nu_i - \nu_j| \leq |J_{ij}|. \tag{3}$$

Even for very small spin-spin couplings (even 0.5 Hz or lower), the condition of strong coupling can be met when the magnetic field is low enough. As a consequence of strong coupling, the spins tend to relax with a common apparent R_1 rate. In this context, it is important to emphasize that the relaxation rates refer to spin states but not to individual spins. In addition, there were sharp features in the NMRD curves found, which are caused by avoided crossings[14, 19–22] of energy levels of the coupled spin system. Both effects can be observed even when the condition of fast motion (extreme narrowing $\omega\tau_c = 1$, consequently, $J(\omega) = $ const.) is fulfilled within the whole field range studied. They are manifest not only for the individual spins but for the coupled spin system as a whole; thus, they become important for the low-resolution NMRD studies as well and must be taken into account for properly analyzing the data.[14, 19] Furthermore, when during the preparation period of the experiment non-thermal polarization is formed, efficient coherent polarization transfer among the strongly coupled spins becomes possible.[20–22]

Effects similar to those observed for proton systems are expected to exist also for protons coupled to spin $\frac{1}{2}$ hetero-nuclei. However, observing such effects is a difficult experimental task. The condition of strong coupling can be relatively easily fulfilled for two protons due to the relatively small span of the proton NMR frequencies. For small differences in chemical shift two protons can be strongly coupled even at fields of several Tesla. However, to fulfill the strong coupling condition for protons and spin $\frac{1}{2}$ nuclei with lower gyromagnetic ratios much lower fields are required: approximately 10 μT for protons and ^{19}F, and even smaller fields for protons and ^{13}C. Thus, at first glance, at higher fields hetero-nuclei should not have any pronounced effect on the spin relaxation of protons because of their weak coupling to protons.

Nonetheless, one can still expect effects of hetero-nuclei under less demanding conditions, namely, when (i) two protons are strongly coupled and (ii) experience spin-spin interactions of different strengths with the hetero-nucleus. In this case the hetero-nucleus modifies the spin eigen-functions differently depending on its spin projection on the magnetic field axis. As a consequence, for different states of the hetero-nucleus different proton NMRD is expected. Verifying this idea both theoretically and experimentally and thus elucidating the role of hetero-nuclei on the proton NMRD is the main concern of the present work. In our experiments, we use ^{19}F as model hetero-spin $\frac{1}{2}$, but the results are directly transferable to any other spin $\frac{1}{2}$ nucleus. In addition, we will consider effects of hetero-nuclei on coherent polarization transfer among strongly coupled protons at low fields. As will be shown, effects of ^{19}F nuclei on proton relaxation and on coherent re-distribution of polarization in the proton spin subsystem are strongly interrelated.

II. EXPERIMENTAL

A. Compounds studied and sample preparation

5-Bromo-2,4-difluoroaniline (BDFA), DCl, and glass distilled deuterated water (D$_2$O) were received from Sigma-Aldrich. The 0.5 ml solution containing 0.1 M of BDFA and 0.85 M of DCl was prepared by dissolution of the compounds in D$_2$O in the NMR-tube without any additional purification. The resulting acidic pH is necessary for solubility of BDFA. All samples were purged with pure nitrogen gas and sealed in a standard 5 mm Pyrex NMR tube. In order to avoid vortex formation and sample shaking during the transfer, a Teflon plug was inserted into the tube on top of the liquid.

B. Field-cycling NMR

A detailed description of the experimental field-cycling setup with probe shuttling between two magnets is given elsewhere.[23–25] This setup allows one to detect high-resolution NMR spectra under permanent slow sample rotation (0–150 Hz) at $B_0 = 7$ T, while for spin evolution a variable field B_{int} in the range from 50 μT to 7 T is used. For 0.1 T $< B_{int} < 7$ T, the field is set by digitally controlled positioning of the probehead with the sample in the stray field of the spectrometer cryomagnet. At fields below 0.1 T, B_{int} is set by control of the electric current through an auxiliary magnetic system placed under the cryomagnet centered at a position where the stray field is 50 mT. The residual field gradient of the stray field along z is compensated by three incorporated coils reducing the field variation over the sample volume to only a few microtesla.

C. Experimental protocol

The NMRD experiments were carried out according to the protocol depicted in Figure 1.[14, 19] The timing scheme of the experiment consists of 5 consecutive stages. At first, the spin system is relaxed to thermal equilibrium during a sufficiently long time, τ_R (far exceeding the relaxation times of the spin system), at the magnetic field B_R and acquires
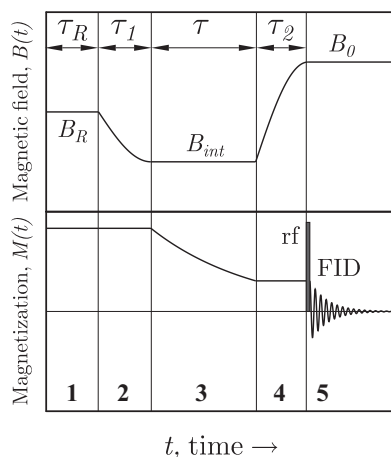
FIG. 1. Timing scheme of the field-cycling experiment. The cycle consists of a relaxation period at field B_R during the time τ_R (stage 1); switching to evolution field B_{int} during time τ_1 (stage 2), a variable delay time τ at this field (stage 3), switching to detection field B_0 during time τ_2 (stage 4), and detection by applying an RF-pulse and recording the FID (stage 5).
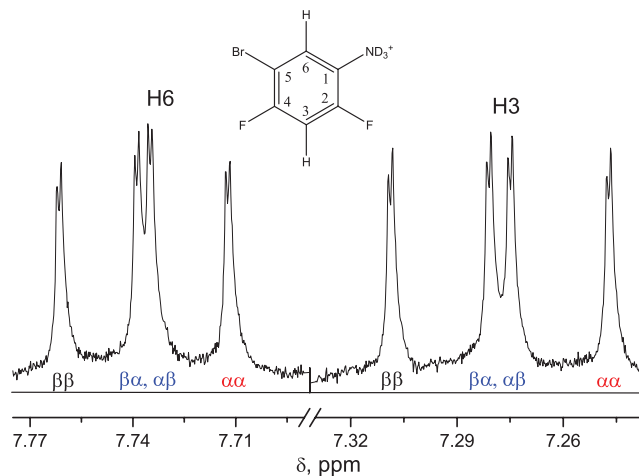

FIG. 2. ^{1}H NMR spectrum and structure of 5-bromo-2,4-difluoroaniline (BDFA) in acidic D$_2$O. Greek letters indicate spin sub-ensembles of the two fluorine atoms.

longitudinal Boltzmann spin magnetization at this field (stage 1). Then, during time, τ_1, the magnetic field is rapidly switched from B_R to the field B_{int} of intermediate strength (stage 2). This is the end of the preparation period. At this point, the spin system starts to relax to a new equilibrium during the variable time interval, τ (stage 3). As the equilibrium longitudinal magnetization is proportional to the external magnetic field and $B_R \neq B_{int}$, there is longitudinal relaxation taking place during stage 3. After this relaxation period, the magnetic field is rapidly switched again during time, τ_2, from B_{int} to the observation field B_0 of the NMR spectrometer (stage 4); here the Fourier transform NMR spectrum is detected (stage 5). At this field, the spins are only weakly coupled and therefore can be studied individually. To obtain the relaxation kinetics, the intensity of the NMR signal of individual spectral lines was studied as function of the variable time interval, τ. The relaxation time, T_1, of the longitudinal relaxation was extracted from such a kinetics by a monoexponential fit (in the case of non-exponential relaxation kinetics, an apparent relaxation time was extracted); finally, the dependence of the extracted T_1-relaxation times on the magnetic field B_{int} constitutes the NMRD curve.

The choice of magnetic field B_R is conditioned by optimization of the signal-to-noise ratio. In the high temperature approximation (valid at ambient temperature), the equilibrium magnetization at a given field is proportional to this field; thus, the maximal change in magnetization during the relaxation process is proportional to $(B_R - B_{int})$. In our experiments, we tried to maximize the amplitude of variation during relaxation at $B = B_{int}$. For this reason, for $B_{int} < B_0/2$ we set $B_R = B_0$ (experiment with magnetization decay at the intermediate field), while for $B_{int} > B_0/2$ we used $B_R = 0$ (magnetization recovery at the field B_{int}). At fields B_{int} close to $B_0/2$ we used both $B_R = 0$ and $B_R = B_0$ and compared the relaxation data to make sure that the relaxation times measured for the two different B_R coincide. Field variation times τ_1 and τ_2 were taken short (the longest field variation time was 290 ms), $\tau_1, \tau_2 \ll T_1$,

so that practically no spin relaxation was taking place during field switching.

Polarization transfer experiments were done in a slightly modified way. At the end of stage 1 at $B_R = B_0 = 7$ T, a selective low amplitude RF pulse was applied to flip the magnetization of only one proton. The rest of the experimental protocol was the same.

III. RESULTS AND DISCUSSION

A. NMRD of protons

The ^{1}H NMR spectrum and the structure of BDFA in D$_2$O are shown in Figure 2. There are two protons coupled to each other; in addition, each of them has coupling to two fluorine atoms. The couplings between fluorine atoms and protons are different for the two protons. These couplings result in splitting the proton signals into four components: the outer components correspond to the $|\alpha\alpha\rangle$ and $|\beta\beta\rangle$ states of the two fluorine spins, whereas the strongly overlapping central components are characterized by the fluorine spin state with zero z-projection, F_z, of their total spin. The NMR parameters (chemical shifts and spin-spin interactions) of the spin system are listed in Table I together with the T_1-relaxation times at high field, $\mathcal{T}_1^i$, which are the relaxation times of the spins in the regime of weak coupling.

TABLE I. NMR parameters of 5-bromo-2,4-difluoroaniline.

	H3	H6	F2	F4
δ (ppm)	7.28	7.74	$\delta_{F4} - \delta_{F2} = 20.05$ ppm	
$\mathcal{T}_1^i$	7 s	35 s	5.3 s at 7 T	6.9 s at 7 T
			11.5 s at $B = 0.1$ mT	11.7 s at $B = 0.1$ mT
			Measured separately in the whole field range	
J (Hz)				
H3	...	0.37	10.1	8.4
H6	0.37	...	8.0	6.8
F2	10.1	8.0	...	8.2
F4	8.4	6.8	8.2	...

For two protons, their apparent T_1-relaxation times coincide when the difference in their precession frequencies, $\delta\nu$, goes to zero. In such a case, the eigen-states of the spin system are the singlet and triplet states. Thus, the coupled spins are fully entangled, which results in their relaxation with a common relaxation time, $T_{av} = 2T_1^1 T_1^2 / (T_1^1 + T_1^2)$.[19,26] When there are only two protons and no other nuclei in the system, the condition $\delta\nu = 0$ is obviously fulfilled at zero magnetic field. Features in the proton NMRD (coincidence of the relaxation times at zero difference in precession frequency) can also be interpreted as a level anti-crossing effect. By level anti-crossing (or avoided crossing) we mean the situation where two or more spin energy levels (corresponding to $|\alpha\beta\rangle$ and $|\beta\alpha\rangle$ states in our case) tend to cross at a certain magnetic field, but the presence of an interaction (J-coupling in our case) results in their "repulsion". Due to the presence of the interaction the spin eigen-functions change (to $|S\rangle$ and $|T_0\rangle$ states in our case) and the energy levels no longer cross, but have a minimum distance $\Delta E > 0$. In the case of the two-spin system $\Delta E = |J|$. At the level anti-crossing point one should always expect pronounced features in the NMRD.[14,19] For the two-spin system, the corresponding feature is the coincidence of the relaxation times of the coupled spins. In fact, the presence of a level anti-crossing always means that spins are strongly coupled and therefore results in distinct features in the field dependence of relaxation and polarization transfer phenomena. As will be shown below, the condition of having an anti-crossing at a certain magnetic field strength is more specific than the condition given by Eq. (3), which in this form is valid only for a pair of spins and changes when all terms in the spin Hamiltonian of a multi-spin system are taken into account.

The presence of ^{19}F nuclei definitively changes the expected behavior of the NMRD, thus the simple considerations presented above are no longer valid. The experiments show that the different NMR spectral components of the two protons relax considerably differently (Figure 3). The NMRD curves were measured individually for different components of the protons multiplets, which are characterized by F_z equal to ± 1 and 0. The proton relaxation dispersions of individual sub-ensembles are shown in Figure 3. It is clearly seen that the spin $\frac{1}{2}$ hetero-nuclei have a strong effect on the proton NMRD curves: not only are the proton relaxation times field-dependent, but they also strongly depend on the spin state of the fluorine atoms, although the ^1H spins are only weakly coupled to the ^{19}F spins (difference between Zeeman interactions of the hetero-nuclei was always much bigger than their spin-spin interaction). Moreover, the expected behavior (coincidence of the proton relaxation times at zero field) is seen only for the ^{19}F states with $F_z = 0$ (Figure 3(c)). However, even for this sub-ensemble there is an additional feature in NMRD at 90 mT. For the molecules in the spin state $|\alpha\alpha\rangle$ of the two ^{19}F atoms, the proton relaxation times do not coincide at any magnetic field (Figure 3(b)), whereas for the $|\beta\beta\rangle$ sub-ensemble of the two ^{19}F atoms, there is a feature (coincidence of the proton T_1-relaxation times) showing up in the proton NMRD curve at 90 mT (Figure 3(a)). The feature at 90 mT also shows up for the other two sub-ensembles; however, it is much less pronounced as compared to the $|\beta\beta\rangle$ sub-ensemble.
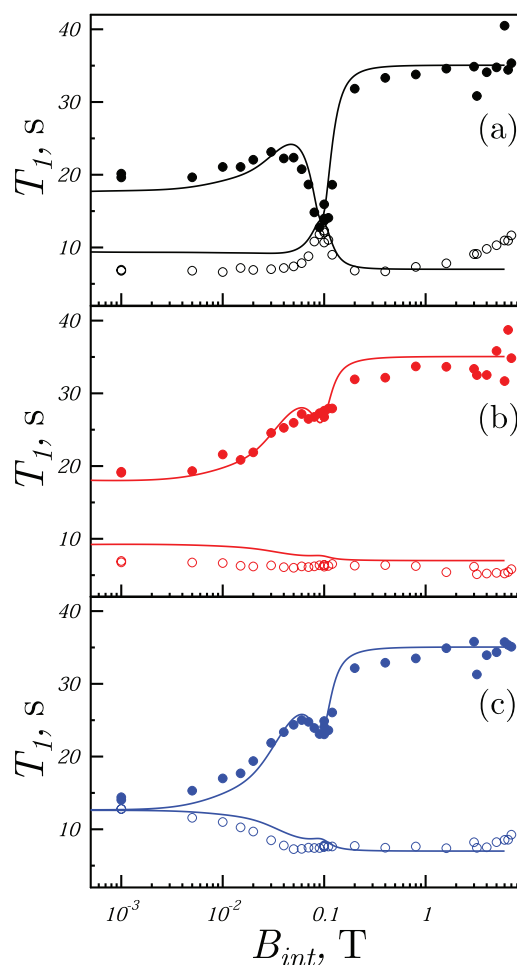
FIG. 3. NMRD of BDFA protons. Experimental data: open circles—H3 proton, filled circles—H6 protons; color relates to the spin state of the ^{19}F atoms: black—$\beta\beta$ sub-ensemble (a), red—$\alpha\alpha$ sub-ensemble (b), blue—$\beta\alpha$, $\alpha\beta$ sub-ensembles (c); simulations are shown by solid lines in the respective color.

The solid lines in Figure 3 show the results of theoretical calculations, which will be explained later in the text.

Thus, the observed NMRD curves are rather different from those in the case of coupled protons in the absence of hetero-nuclei. Before performing theoretical calculations let us first discuss on a qualitative level why such effects of ^{19}F on the proton NMRD are seen in the limit of weak coupling between the ^1H and ^{19}F spins.

As has been mentioned above, the condition $\delta\nu = 0$ of strongest coupling and, consequently, of level anti-crossing is usually fulfilled at zero magnetic field in accordance with Eq. (3). However, the situation changes when more spins are coupled and all spin-spin interactions are considered. In particular, in the presence of a spin $\frac{1}{2}$ hetero-nucleus each proton experiences a magnetic field equal to $2\pi J_{iF}F_z/\gamma_H$ (γ_H is the proton gyromagnetic ratio) in addition to the external field. Here J_{iF} is the J-coupling of the i-th proton spin to the hetero-nucleus; F_z is the z-projection of the spin of the hetero-nucleus ($-\frac{1}{2}$ or $\frac{1}{2}$). Thus, the frequency difference is as follows:

$$\delta\nu = \gamma_H B(\delta_1 - \delta_2)/2\pi - (J_{1F} - J_{2F})F_z. \tag{4}$$

Here $(\delta_1 - \delta_2)$ is the chemical shift difference of the two protons. As a result, the condition $\delta\nu = 0$ is fulfilled when the following conditions are met:

$$\gamma_H B(\delta_1 - \delta_2)/2\pi = (J_{1F} - J_{2F})F_z. \qquad (5)$$

When $\delta J = (J_{1F} - J_{2F}) \neq 0$ the field strength B, at which the equality $\delta\nu = 0$ is fulfilled, is non-zero. As a consequence, for one ^{1}H spin sub-ensemble the T_1-relaxation times coincide at $B = |2\pi(J_{1F}-J_{2F})F_z/\gamma_H(\delta_1-\delta_2)|$, whereas for the other sub-ensemble with opposite F_z there is no such field position as $\gamma_H B(\delta_1 - \delta_2)/2\pi$ and $(J_{1F} - J_{2F})F_z$ have opposite signs. Thus, the presence of unequal couplings of protons with the hetero-nucleus moves the level anti-crossing and the corresponding feature in NMRD away from zero field; depending on the F_z value the resulting NMRD curve will be considerably different. Relation (5) means that hetero-nuclei can affect the proton NMRD even in the limit of weak proton-fluorine coupling, when the following conditions are met: (i) the protons are strongly coupled with each other and (ii) they have different spin-spin interaction constants, J_{1F} and J_{2F}, with the hetero-nucleus. Such conditions are much less demanding than strong coupling of the protons with the hetero-nuclei and can be met even at high fields of the order of several Tesla. Other spin $\frac{1}{2}$ nuclei, e.g., ^{13}C, ^{15}N, ^{31}P, affect the proton NMRD in the same way.

To illustrate in more detail the effects of hetero-nuclei on proton NMRD, we performed a numerical simulation for a two-proton system coupled to two hetero-nuclei. When modeling the experimental results, we will assume that the dynamic evolution of the spin system (which also defines the spin eigen-states of the molecule) is described by the following Hamiltonian:

$$\hat{H} = 2\pi\left(-\sum_{i=1}^{N} \nu_{Hi}\hat{I}_{iz} + \sum_{i<j}^{N} J_{ij}(\hat{\mathbf{I}}_i \cdot \hat{\mathbf{I}}_j) - \sum_{k=1}^{N'} \nu_{Fk}\hat{F}_{kz}\right.$$
$$\left. + \sum_{k<l}^{N'} J_{FkFl}(\hat{\mathbf{F}}_k \cdot \hat{\mathbf{F}}_l) + \sum_{i,k}^{N,N'} J_{iFk}\hat{I}_{iz}\hat{F}_{kz}\right). \qquad (6)$$

Here N protons and N' hetero-nuclei are considered with the precession frequencies, $\nu_{Hi} = \gamma_H B(1 + \delta_i)/2\pi$ and $\nu_{Fk} = \gamma_F B(1 + \delta_{Fk})/2\pi$, with δ_{Fk} being the chemical shift of the k-th hetero-nucleus; J-couplings between all pairs of protons, J_{ij}, and all pairs of hetero-nuclei, J_{FkFl}, are considered as well as those between protons and hetero-nuclei, J_{iFk}. For the coupling between the protons and fluorine atoms only the secular parts of the spin-spin interactions are taken, since always the regime of weak coupling is given: for proton and fluorine Eq. (3) is fulfilled only at $B < 10\,\mu$T, whereas in the experiments only fields above 0.1 mT were used.

Spin relaxation is assumed to be due to fluctuations of the local field experienced by protons and hetero-nuclei, respectively. Although such an approach is rather simplified, it well reproduces the main features of relaxation in the coupled spin systems. To calculate the rates of the relaxation transitions between the spin levels Redfield theory[27] was used. When needed, more complex relaxation mechanisms (e.g., due to modulation of intra-molecular dipole-dipole interactions) can be taken into account. However, they require a more precise

knowledge of the molecular structure (chemical bond lengths and angles between the bonds) and will not be considered here. For the sake of simplicity we will also consider only relaxation of the populations of the spin energy levels, thus significantly reducing the dimension of the relaxation matrix $\hat{R}$ (which is originally a super-operator) and neglecting many matrix elements. Limitations of such an approximation, which is valid when $J_{12}T_1^i > 1$, have been discussed in detail in our previous works.[14,19] Also, the method of calculating the apparent T_1-relaxation times is the same as previous one.[14,19] Finally, we will assume that field variation from B_{int} to B_0 is sudden for the coupled spins, so that the field switching does not affect the apparent relaxation times. This approximation is physically reasonable because of the very small coupling of 0.37 Hz between the two protons in the compound considered here. Effects of the field switching speed on the relaxation rates observed at high field have also been discussed in detail earlier[19] and can, in principle, be taken into account in the approach developed.
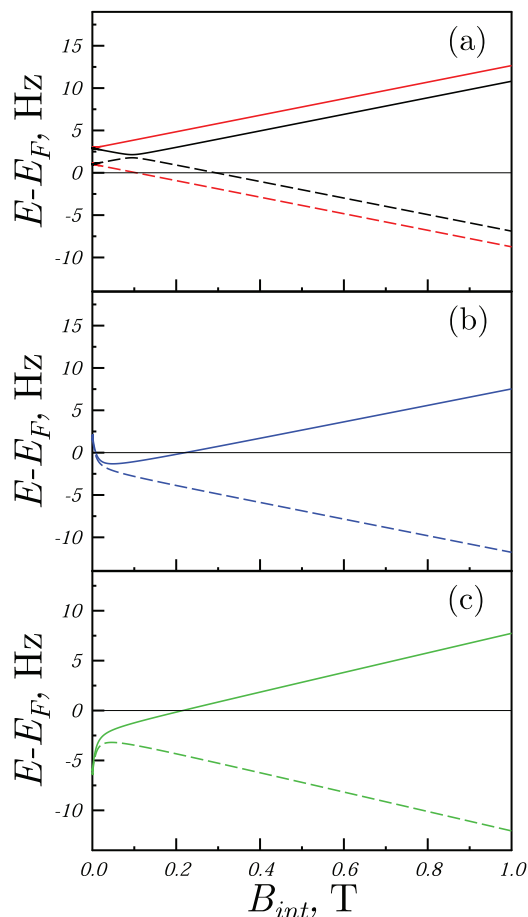

FIG. 4. Energies of the spin levels of two coupled protons characterized by $I_z = 0$ when the hetero-nuclei are in states $|\beta\beta\rangle$ (black) and $|\alpha\alpha\rangle$ (red) (subplot a); and when they are characterized by $F_z = 0$ (blue and green) (subplots b and c). Parameters of calculation were taken from Table I; for convenience we subtracted the large fluorine energy, E_F, from the total energy. Solid and dashed lines show the energies of the protons spin states, which correspond to the high-field $\alpha_{H3}\beta_{H6}$ and $\beta_{H3}\alpha_{H6}$ states, respectively. Blue and green curves correspond to the energies of fluorine spin states, which go to the high-field $\beta_{F2}\alpha_{F4}$ and $\alpha_{F2}\beta_{F4}$ states, respectively.
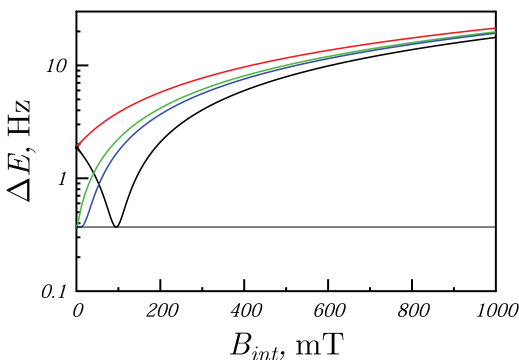
FIG. 5. Splitting, ΔE, between pairs of coupled spin levels shown in Figure 4 when the hetero-nuclei are in states $|\beta\beta\rangle$ (black) and $|\alpha\alpha\rangle$ (red); and in states with $F_z = 0$ (blue and green lines). Thin solid line shows the minimal possible splitting between the levels equal to $J_{12} = 0.37$ Hz. Color coding of the ^{19}F spin states is the same as in Fig. 4.

The energies of the proton spin levels in BDFA characterized by $I_z = 0$ for different states of the hetero-nucleus are shown in Figure 4. The energy differences, ΔE, for these pairs of states are shown in Figure 5. Such states coincide with the proton $|\alpha\beta\rangle$ and $|\beta\alpha\rangle$ states in the limit of weak coupling, while for the strong coupling regime they represent their superposition. Level anti-crossings are clearly seen at $B \neq 0$ for one spin sub-ensemble with parallel spins of the hetero-nuclei (Figure 4(a)) and at $B = 0$ for the spin sub-ensembles with the fluorine spin states characterized by $F_z = 0$ (Figures 4(b) and 4(c)). When the spins of the hetero-nuclei are in the $|\alpha\alpha\rangle$ or $|\beta\beta\rangle$ states that are eigen-states of $\hat{H}$, $\delta\nu$ is as follows:

$$\delta\nu = \frac{\gamma_H B(\delta_1 - \delta_2)}{2\pi} \pm \frac{(J_{1F1} - J_{2F1}) + (J_{1F2} - J_{2F2})}{2}. \tag{7}$$

As a consequence, the level crossing is seen at the following field:

$$B_{lac} = \pi \left| \frac{(J_{1F1} - J_{2F1}) + (J_{1F2} - J_{2F2})}{\gamma_H(\delta_1 - \delta_2)} \right|. \tag{8}$$

At this field for one of the hetero-nuclear spin sub-ensembles ($|\beta\beta\rangle$ in the BDFA case) the proton spin energy levels exhibit an anti-crossing (Figure 4(a)), whereas for the other ensemble (namely, when $\gamma_H B(\delta_1 - \delta_2)$ and $(J_{1F1} - J_{2F1})F_{1z} + (J_{1F2} - J_{2F2})F_{2z}$ are of the same sign, $|\alpha\alpha\rangle$ in our case as shown in Figure 4(a)) there is no such feature. At the anti-crossing field the splitting of the proton spin energy levels with $I_z = 0$ is equal to the proton-proton coupling, J_{12} (Figure 5). In such a simple case it is sufficient to calculate the proton spin energy levels for only one spin sub-ensemble of the hetero-nuclei, while for all the others they can be obtained by simply shifting the calculated energy levels along the abscissa. However, when the fluorine spin states are characterized by $F_z = 0$ the Hamiltonian (6) cannot be solved analytically if $J_{1F2F} \neq 0$; then the eigen-states of the system are not given by pure product functions $|\alpha\beta\rangle$ and $|\beta\alpha\rangle$ of the fluorine spins, but by a superposition. However, as a simple estimate we can assume that in this case the protons experience an almost vanishing field of the fluorine atoms; hence the position of the level crossing and, consequently, of the feature in the proton NMRD occurs at $B \approx 0$. This estimate

agrees with the numerical calculation of the spin energy levels (Figures 4(b), 4(c), and 5): the splitting of the proton energy levels is minimal at zero field, the minimal splitting perfectly coincides with J_{12}. In principle, also for the states characterized by $F_z = 0$ the level anti-crossings can move away from zero field. For instance, this is the case when the fluorine-fluorine coupling is zero, $J_{1F2F} = 0$, so that the $|\alpha\beta\rangle$ and $|\beta\alpha\rangle$ states of the hetero-nuclei are the eigen-states of the Hamiltonian (6). Then an equation similar to Eq. (8) can be used to find the positions of the level anti-crossing for protons. When $(J_{1F1} - J_{2F1}) \neq (J_{1F2} - J_{2F2})$, the feature corresponding to the $|\alpha\beta\rangle$ and $|\beta\alpha\rangle$ states of the hetero-nuclei is no longer located at $B = 0$ but exhibits a more complex behavior: for one of the sub-ensembles it shifts to a positive field where $|\frac{\gamma_H B(\delta_1 - \delta_2)}{2\pi}| = |\frac{(J_{1F1} - J_{2F1}) - (J_{1F2} - J_{2F2})}{2}|$, whereas for the other sub-ensemble it disappears.

The calculated field dependences of the relaxation times of BDFA for different F_z sub-ensembles are shown in Figure 6(a). For simplicity, we assume here that the hetero-nuclei do not relax, so that mixing between the ensembles of different F_z does not occur. This condition implies that the T_1-relaxation times of the hetero-nuclei are much longer than the proton relaxation times and $1/J_{12}$. The calculation fully confirms our expectations: the apparent relaxation times coincide at distinctive field strengths where $\delta\nu = 0$ for the spin ensemble chosen. The positions of such fields, B_{lac}, for the $|\alpha\alpha\rangle$ and $|\beta\beta\rangle$ sub-ensembles of the fluorine spins are given by Eq. (8). Thus, for the $|\beta\beta\rangle$ sub-ensemble of the hetero-nuclei there is a feature at $B_{lac} \approx 90$ mT in the proton NMRD: at this field the relaxation times of the corresponding spectral components coincide. For the $|\alpha\alpha\rangle$ sub-ensemble there is no such feature: the proton relaxation times do not coincide at any field. For the $F_z = 0$ states of the hetero-nuclei the feature in the proton NMRD is at zero field.

Thus, depending on the spin state of the fluorine atoms we expect to have different proton NMRD with features (coincidence of the proton T_1-relaxation times) at different magnetic fields: 90 mT and zero field. The experimental data (Figure 3) qualitatively agree with these expectations: the positions of the features are well reproduced by our simple estimates following from the condition, $\delta\nu = 0$. However, such a simplified description cannot reproduce certain peculiarities of the NMRD curves. Namely, the features in NMRD, which correspond to the level anti-crossing of one particular sub-ensemble, also reveal themselves for the other sub-ensembles as can be seen from Figure 3. For instance, the feature at 90 mT is predominant for the $|\beta\beta\rangle$ sub-ensemble; however, it is also present for the other spin sub-ensembles, but cannot be reproduced by a simple model neglecting fluorine spin relaxation. In particular, the results for different sub-ensembles cannot be obtained from each other by shifting the corresponding NMRD curves along the abscissa. Therefore, for the quantitative description of the observed NMRD a more elaborate model is needed. To model the experimental data it is necessary to take the fluorine T_1-relaxation into account, which results in the exchange of proton spin magnetization between the different sub-ensembles. Hence, relaxation of the ^{19}F nuclei was measured independently in the whole field range studied. The field-dependent T_1-relaxation
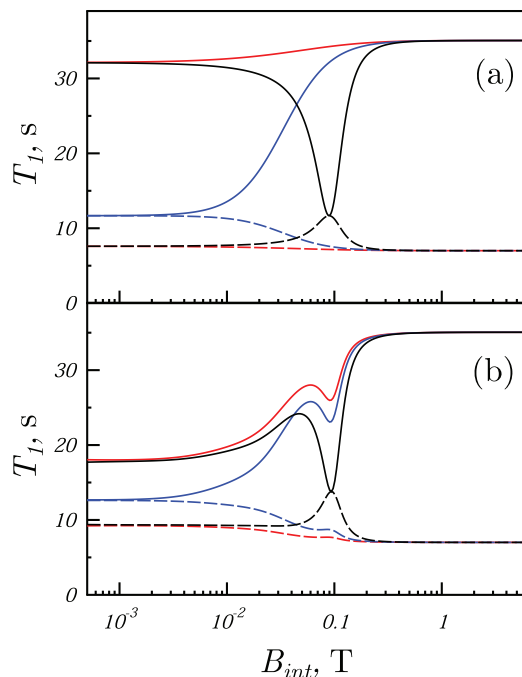
FIG. 6. Calculated NMRD curves for BDFA protons in the absence (a) and in the presence (b) of ^{19}F spin relaxation; dashed lines—H3 proton, solid lines—H6 protons; color indicates the spin state of ^{19}F atoms: black—$\beta\beta$ sub-ensemble, blue—$\beta\alpha, \alpha\beta$ sub-ensembles, red—$\alpha\alpha$ sub-ensemble. Parameters of calculation were taken from Table I.

times of the fluorine atoms were introduced in the calculation, whereas more subtle effects of cross-correlation[28, 29] between ^{1}H and ^{19}F spins were neglected. Calculation in such approximation using the Hamiltonian (6) and taking ^{19}F relaxation into account (solid lines in Figure 3) perfectly describes the experimental data: exchange effects between different ^{19}F spin sub-ensembles in the proton NMRD are well reproduced. As a consequence, the feature at 90 mT is most pronounced for the $|\beta\beta\rangle$ sub-ensemble (as follows from the simple estimate $\delta\nu = 0$) but can also be seen for the other sub-ensembles, although it has a lower amplitude. Likewise, in order to reproduce the NMRD around $B \approx 0$, consideration of the ^{19}F relaxation is also necessary. Thus, the improved theoretical model can well reproduce the NMRD for all individual sub-ensembles.

A comparison of the simplified model (no relaxation of ^{19}F nuclei) and the extended model (fluorine relaxation is taken into account) is presented in Figure 6. It is clearly seen that the simplified model (Figure 6(a)) can only reproduce the positions of the features in NMRD but predicts considerably differing NMRD curves. In the simplified model the features coming from the level anti-crossings are seen only for the corresponding sub-ensemble, in which the level crossing is present. This is the case not only for the feature at 90 mT but also for that at zero field. In the simplified model at $B \approx 0$, the difference in T_1 for individual protons in the $|\alpha\alpha\rangle$ and the $|\beta\beta\rangle$ sub-ensembles of the ^{19}F spins is much larger than in the extended model. Fluorine spin relaxation, which mixes different sub-ensembles, is the cause of this discrepancy. The improved model (Figure 6(b)) taking fluorine relaxation into

account can describe the exchange between different ^{19}F spin sub-ensembles and fits well the experimental data (Figure 3).

It is worth noting that protons can also affect the NMRD of the hetero-nuclei in the same way. However, features in the NMRD of protons and hetero-nuclei are located at different magnetic fields because the characteristic chemical shift values are usually considerably different for the nuclei of different kinds. While for protons $(\delta_i - \delta_j)$ are rarely larger than a few ppm, the range of chemical shift can be several hundred ppm for instance, for ^{19}F or ^{13}C nuclei. As a consequence, the features in NMRD of hetero-nuclei are expected to be shifted to much lower fields according to Eq. (8); the smaller gyromagnetic ratio of hetero-nuclei, which shifts the features in the opposite direction, can only partly compensate this effect. However, in the case under study we did not find any features in the ^{19}F NMRD because the intrinsic T_1-relaxation times, $\mathcal{T}_1^i$, of the fluorine spins coincide already in the weak coupling regime. Therefore, spin-spin interactions do not affect the ^{19}F NMRD curves in our case.

B. Polarization transfer between protons

Our previous theoretical studies and also the analysis of the NMRD measured in model systems[14, 19] show that taking into account only relaxing state populations can be rather restricting and that evolution of coherences between the spin states has to be included into consideration. This is because spin relaxation proceeds not only through state populations relaxing to their equilibrium values, but also via coherences. Effects of spin coherences are particularly pronounced when the system is not at thermal equilibrium at $B = B_R$ prior to the first field jump. Creating a non-equilibrium spin system is done in the easiest way by applying an appropriate pulse sequence, which selectively flips only certain spins. Another necessary condition for having coherence at $\tau = 0$ is non-adiabatic field switching, because it can transfer state population differences at high field into coherences at low field.[14, 19–21] In this case the spin system starts evolving from a coherent state. Then not only relaxation is taking place but also the polarization transfer among the strongly coupled spins.[14, 19–21] In the present work, we will once again demonstrate this effect showing in particular that when setting a proper magnetic field B_{int} one can observe a polarization transfer between the coupled protons, which is selective with respect to the spin state of fluorine spins.

The experiments were done according to the protocol shown in Figure 1 with the following addition. First the spin system was equilibrated at $B = 7$ T, then a selective low amplitude π-pulse was applied to invert the magnetization of only proton H3. Thus, prior to the first field switching the H6 proton has positive z-magnetization, whereas the H3 proton has negative net polarization. The following field switches were sudden in all cases, since the J-coupling between protons was very small on the timescale of the experiment. The magnetic field B_{int} was varied to observe the selectivity of polarization transfer.

The idea of polarization transfer is as follows:[13, 14, 19] First, at high magnetic field the two states of protons H3 and

H6, $|\alpha\beta\rangle$ and $|\beta\alpha\rangle$, have different populations, $p_{\alpha\beta}$ and $p_{\beta\alpha}$, due to a suitable preparation. Such a population pattern can be prepared, as in our case, by applying selective RF pulses, which affect the NMR lines of only one spin, to initially thermally polarized molecules. Another way is creating spin hyperpolarization, which usually is spin-selective.[30] Second, when the field B_{int} corresponds to the position of the level anti-crossing the population difference $(p_{\alpha\beta} - p_{\beta\alpha})$ can be efficiently transformed into a coherence at $B = B_{int}$. This is the case when the field switching is sudden and relaxation effects during the switching are negligible. In this situation one obtains the density matrix, ρ, at $B = B_{int}$ by projecting the initial density matrix at the high field B_0 onto the new eigen-basis at $B = B_{int}$, which is the singlet-triplet basis. As a consequence, we obtain the following expressions for the state populations, p_i (diagonal elements of the density matrix) and coherences ρ_{ij} (off-diagonal elements of the density matrix) at $B = B_{int}$:

$$p_S = \rho_{SS} = \frac{p_{\alpha\beta} + p_{\beta\alpha}}{2}, \quad p_{T_0} = \rho_{T_0 T_0} = \frac{p_{\alpha\beta} + p_{\beta\alpha}}{2},$$

$$\rho_{S T_0} = \rho_{T_0 S} = \frac{p_{\alpha\beta} - p_{\beta\alpha}}{2}. \tag{9}$$

Thus, in the ideal case (sudden switching and very slow spin relaxation) the two eigen-states at B_{int}, $|S\rangle$ and $|T_0\rangle$, have equal populations, and, in addition, a coherence between states $|S\rangle$ and $|T_0\rangle$ is formed, proportional to the initial population difference. This coherence is the main cause of spin evolution in the system. Once formed, the spin coherence starts oscillating with a frequency equal to the splitting between the two levels (proton spin-spin coupling in the case under study). When the second field switching to the detection field is also sudden, the coherence will be transferred back into a population difference, which is directly monitored by the NMR line intensity. As a result, the NMR signal when measured as a function of τ contains a pronounced oscillating component. By varying the delay τ one can efficiently manipulate the polarization transfer between the coupled protons and transfer net polarization from one spin to the other.

A new feature of the system containing hetero-nuclei as compared to the simpler isolated two-proton system studied earlier[14, 19] is that there are several level anti-crossings in the system, which are well separated from each other in their positions. Importantly, each level anti-crossing position corresponds to a certain state of the ^{19}F spins, i.e., to particular lines in the proton NMR spectrum. Thus, using the same concept as before[14, 19] it is possible to transfer non-thermal polarization between selected lines in the ^{1}H NMR spectrum.

Experimental results illustrating the polarization transfer among selected lines within the multiplets in the proton NMR spectrum are presented in Figure 7. We are able to observe coherent polarization transfer, which proceeds only between particular lines of the proton multiplets depending on the magnetic field value. Here two magnetic fields, $B_{int} = 0.1$ mT and 85 mT, corresponding to two features shown in Figures 3(a) and 3(c) are chosen. While the lines of the multiplets that are not affected by polarization transfer relax exponentially with their T_1s, there are groups of lines that have an oscillatory component. At 0.1 mT (Figure 7(a)) the two central groups of lines of each proton multiplet corresponding to
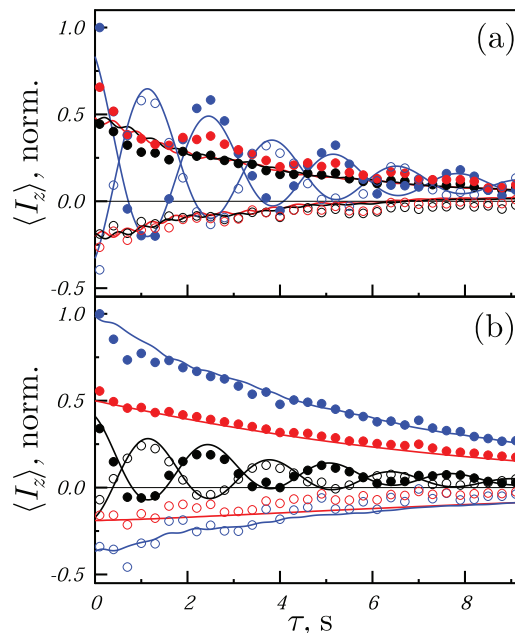

FIG. 7. Kinetics of polarization transfer of BDFA protons at 0.1 mT (a) and 85 mT (b) after a selective inversion of H3 proton magnetization at $B_R = 7$ T. Polarization is normalized to the largest value. Open circles —H3 proton, filled circles—H6 proton; color indicates spin state of the fluorine atoms in the same way as in Figure 3: $|\beta\beta\rangle$ (black), $|\alpha\alpha\rangle$ (red), and $|\alpha\beta\rangle$ or $|\beta\alpha\rangle$ (blue). Simulations are shown as solid lines with corresponding color.

the $F_z = 0$ spin states of ^{19}F undergo polarization transfer, whereas at 85 mT (Figure 7(b)) the components of the multiplets corresponding to the $|\beta\beta\rangle$ spin state of ^{19}F are affected. Thus, coherent polarization transfer takes place only for those spin sub-ensembles, for which there is a level anti-crossing at $B = B_{int}$; proper choice of B_{int} at a particular level crossing leads to polarization transfer selectively between the corresponding components in the proton NMR spectrum.

The polarization transfer kinetics was described quantitatively by numerically solving the Liouville equation for the density matrix of the four-spin system. We have taken into account the dynamic spin evolution described by the Hamiltonian $\hat{H}$ from Eq. (6) and the relaxation given by the super-operator $\hat{\hat{R}}$; we assumed that the field variation was sudden. The details of this approach are given in Refs. 14 and 19. The calculated polarization transfer kinetics is in perfect agreement with the experimental data. It is worth noting that the only fitting parameters were the initial signal intensities for $\tau = 0$, while NMR parameters and relaxation times were taken from Table I. The calculation perfectly reproduces the quantum oscillations and damping caused by spin relaxation. As the magnetic fields were set to the level anti-crossing fields ($B_{lac} = 0.1$ mT and 85 mT) in the corresponding sub-ensembles of molecules, the frequencies of oscillations observed perfectly fit to the scalar coupling constant, $J_{12} = 0.37$ Hz, between the protons.

Thus, the presence of hetero-nuclei not only affects the NMRD but also allows one to manipulate coherent polarization transfer in the proton spin subsystem by choosing an appropriate level crossing, which corresponds to a particular

spin state of the ^{19}F nuclei. The effects of ^{19}F nuclei on both phenomena, proton relaxation and polarization re-distribution in the proton system, are strongly interrelated and reveal themselves under the same conditions.

IV. CONCLUSIONS

Our studies illustrate the importance of scalar spin-spin interaction in NMRD studies. Here we have shown that not only the homo-nuclear couplings are of importance, but also the couplings to hetero-nuclei; although the regime of strong coupling, $J \ll \delta\nu$ between protons and ^{19}F nuclei is not met in our experiments. Nonetheless, the presence of hetero-nuclei causes pronounced features. Each feature is predominantly observed only for a particular spin state of the hetero-nuclei; the position of the features for different states can be significantly different. The features are explained theoretically by the presence of level anti-crossings for the coupled protons, whose positions differ depending on the eigen-states of the hetero-nuclei. The experimental proton NMRD curves are well reproduced by the theoretical calculation; the field positions of the features are in good agreement with the measurements. Even more subtle effects of the proton spin magnetization exchange between different spectral components are reproduced, which are caused by the T_1-relaxation of the ^{19}F nuclei. Although all the data were obtained for coupled protons and ^{19}F nuclei, the reported effects have a more general nature and appear for spin $\frac{1}{2}$ hetero-nuclei of any other kind.

Our analysis shows that one should be extremely careful with interpreting the NMRD data in the presence of spin $\frac{1}{2}$ hetero-nuclei. In particular, when ^{13}C, ^{15}N, and ^{31}P nuclei are present, which are known to have strong scalar couplings to protons often exceeding 100 Hz, or when dipolar couplings are not completely averaged out, the discussed features in NMRD can shift to considerably higher fields up to several Tesla. The presence of hetero-nuclei affects not only T_1 but also T_2-relaxation times, since for coupled spin systems both relaxation times depend on the relation between J and $\delta\nu$ (namely, on the "mixing angle" of the system defined as $\theta = \frac{1}{2} \arctan(\frac{J}{\delta\nu})$),[26] while $\delta\nu$ is in its turn dependent on the spin state of the hetero-nuclei. Different pairs of coupled spin $\frac{1}{2}$ nuclei are expected to affect the NMRD curve of each partner differently because of their difference in gyromagnetic ratio and range of chemical shifts.

In addition, we have shown that switching to a magnetic field where strong coupling between the protons takes place allows one to observe efficient and coherent polarization transfer. When hetero-nuclei are present in the spin system one can by setting the magnetic field properly choose the appropriate level anti-crossing and thus transfer polarization selectively between certain lines in the proton NMR spectrum. This method can be useful for enhancing particular NMR signals of choice. The same idea can be utilized for other methods of preparing non-equilibrium polarization, for instance, in experiments involving parahydrogen induced polarization (PHIP) (Ref. 31) where the *para*-H$_2$ is attached to a molecule with a spin $\frac{1}{2}$ hetero-nucleus.[32, 33] Setting properly the mag-

netic field B_{int}, namely $B_{int} = B_{lac}$, one can form distinctive spin orders in an optimal way.

[1] I. Bertini, Y. K. Gupta, C. Luchinat, G. Parigi, C. Schlörb, and H. Schwalbe, Angew. Chem., Int. Ed. **44**, 2223 (2005).
[2] I. Bertini, C. Luchinat, and G. Parigi, Adv. Inorg. Chem. **57**, 105 (2005).
[3] D. Canet, Adv. Inorg. Chem. **57**, 3 (2005).
[4] R. B. Clarkson, Top. Curr. Chem. **221**, 201 (2002).
[5] R. Kimmich and E. Anoardo, Prog. Nucl. Magn. Reson. Spectrosc. **44**, 257 (2004).
[6] G. Kothe and J. Stohrer, *The Molecular Dynamics of Liquid Crystals*, NATO ASI Series, Series C (Kluwer, Dordrecht, 1994), p. 195.
[7] C. Luchinat and G. Parigi, J. Am. Chem. Soc. **129**, 1055 (2007).
[8] M. F. Roberts, Q. Cui, C. J. Turner, D. A. Case, and A. G. Redfield, Biochemistry **43**, 3637 (2004).
[9] L. Calucci and C. Forte, Prog. Nucl. Magn. Reson. Spectrosc. **55**, 296 (2009).
[10] B. V. N. Phani Kumar, V. Satheesh, K. Venu, V. S. S. Sastry, and R. Dabrowski, Chem. Phys. Lett. **482**, 239 (2009).
[11] R. G. Bryant and J.-P. Korb, Magn. Reson. Imaging **23**, 167 (2005).
[12] J. Kowalewski and L. Mäler, *The Series in Chemical Physics* (CRC, Taylor & Francis Group, Boca Raton, FL., 2006), p. 426.
[13] A. S. Kiryutin, K. L. Ivanov, A. V. Yurkovskaya, and H.-M. Vieth, Solid State Nucl. Magn. Reson. **34**, 142 (2008).
[14] S. E. Korchak, K. L. Ivanov, A. V. Yurkovskaya, and H.-M. Vieth, J. Chem. Phys. **133**, 194502 (2010).
[15] D. Ivanov and A. Redfield, Z. Naturforsch., A: Phys. Sci. **53**, 269 (1998).
[16] A. G. Redfield, Magn. Reson. Chem. **41**, 753 (2003).
[17] M. F. Roberts and A. G. Redfield, Proc. Natl. Acad. Sci. U.S.A. **101**, 17066 (2004).
[18] M. F. Roberts and A. G. Redfield, J. Am. Chem. Soc. **126**, 13765 (2004).
[19] K. L. Ivanov, A. V. Yurkovskaya, and H.-M. Vieth, J. Chem. Phys. **129**, 234513 (2008).
[20] K. L. Ivanov, K. Miesel, A. V. Yurkovskaya, S. E. Korchak, A. S. Kiryutin, and H. M. Vieth, Appl. Magn. Reson. **30**, 513 (2006).
[21] K. L. Ivanov, A. V. Yurkovskaya, and H.-M. Vieth, J. Chem. Phys. **128**, 154701/1 (2008).
[22] K. Miesel, K. L. Ivanov, A. V. Yurkovskaya, and H. M. Vieth, Chem. Phys. Lett. **425**, 71 (2006).
[23] S. Grosse, F. Gubaydullin, H. Scheelken, H.-M. Vieth, and A. V. Yurkovskaya, Appl. Magn. Reson. **17**, 211 (1999).
[24] S. Grosse, A. V. Yurkovskaya, J. Lopez, and H.-M. Vieth, J. Phys. Chem. A **105**, 6311 (2001).
[25] S. E. Korchak, Ph.D. dissertation , Freie Universität, Berlin, 2010.
[26] R. Freeman, S. Wittekoek, and R. R. Ernst, J. Chem. Phys. **52**, 1529 (1970).
[27] A. G. Redfield, Adv. Magn. Reson. **1**, 1 (1966).
[28] A. Kumar, R. Christy Rani Grace, and P. K. Madhu, Prog. Nucl. Magn. Reson. Spectosc. **37**, 191 (2000).
[29] M. Goldman, J. Magn. Reson. **60**, 437 (1984).
[30] K. Miesel, K. L. Ivanov, T. Köchling, A. V. Yurkovskaya, and H. M. Vieth, Appl. Magn. Reson. **34**, 423 (2008).
[31] J. Natterer and J. Bargon, Prog. Nucl. Magn. Reson. Spectrosc. **31**, 293 (1997).
[32] S. Aime, R. Gobetto, F. Reineri, and D. Canet, J. Magn. Reson. **178**, 184 (2006).
[33] J. Natterer, O. Schedletzky, J. Barkemeyer, J. Bargon, and S. J. Glaser, J. Magn. Reson. **133**, 92 (1998).